

INFLUENCE OF THE ATS OPTICS ON INTRA-BEAM SCATTERING FOR HL-LHC

M. Schaumann*, CERN, Geneva, Switzerland and RWTH Aachen, Aachen, Germany
R. Bruce, J.M. Jowett, CERN, Geneva, Switzerland

Abstract

In the future High Luminosity (HL-)LHC the influence of intra-beam scattering (IBS) will be stronger than in the present LHC, because of higher bunch intensity, small emittance and new optics. The new ATS-optics scheme [1] modifies the lattice in the arcs around the main interaction points (IP) to provide β^* values as small as 0.15 m at the IP but these modifications affect the IBS growth rates. In this paper proton IBS emittance growth rates are calculated with MADX [2] and the Collider Time Evolution (CTE) program [3] for two ATS-optics versions, different settings of the crossing angles and required corrections and various beam conditions at injection (450 GeV) and collision (7 TeV) energy. CTE simulations of the expected luminosity, intensity, emittance and bunch length evolution during fills are also presented.

HL-LHC AND ATS-OPTICS

For the LHC upgrade, the HL-LHC (High Luminosity Large Hadron Collider), very high bunch intensities N_b combined with small emittances ε are necessary to reach the desired high luminosities \mathcal{L} ,

$$\mathcal{L} = \frac{N_b^2 f_0 k_b}{4\pi\beta^*\varepsilon} \sqrt{1 + \left(\frac{\theta_c \sigma_z}{2\sqrt{\varepsilon\beta^*}}\right)^2}, \quad (1)$$

where f_0 is the revolution frequency, k_b the number of colliding bunches, β^* the β -function at the interaction point (IP), θ_c the crossing angle, σ_z the bunch length. The second factor describes the geometric reduction of the luminosity introduced by the crossing angle. A summary of the beam parameters for the case of 25 ns or 50 ns bunch spacing underlying the calculations in this paper is given in Table 1, a list of the official parameters can be found in [4]. The official choice of β^* is 0.15 m in combination with a half-crossing angle of 295 mrad, which differs from the values given in Table 1. Here $\beta^* = 0.1$ m with a corresponding half-crossing angle of 360 mrad was used as a baseline to treat the extreme case.

According to (1) the luminosity can be improved further by reducing the β -function at the IP. However, as β^* is reduced the β -function in the inner triplets, which are the first magnets before and after the IP, rises, leading to aperture and magnet strength limits. The ATS (Achromatic Telescopic Squeezing) scheme [1] uses the matching quadrupoles from the neighbouring interaction regions (IR), in addition to those located nearby, for a *telescopic*

squeeze to further reduce β^* . As Figure 1 shows, this drastically increases the maximum value of β in the enclosed arcs. Note that the plot was cut at $\beta = 1000$ m, but actually reaches about 24 km around the main IPs ($s_{IP1} = 0$ m, $s_{IP5} = 13329$ m) for $\beta^* = 0.1$ m. The procedure is *achromatic* since the sextupole strengths are kept constant, while the peak β -function in the arcs increases. The chromaticity, generated by the low- β triplets, is corrected more efficiently by ensuring a phase advance of $\pi/2$ in the neighbouring sectors. Within the sequence of optics that occur in the squeeze, this feature emerges only at $\beta^* = 0.4$ m; above that value the optics are basically identical with the standard ones, as currently used in the LHC.

Table 1: HL-LHC Beam Parameters

Parameter		25 ns	50 ns
E	[TeV]	7	7
β^*	[m]	0.1	0.1
N_b	[10^{11} charges]	2.2	3.0
$\varepsilon_n = \varepsilon\gamma$	[$\mu\text{m rad}$]	2.5	3.0
ε_l	[eVs]	2.5	2.5

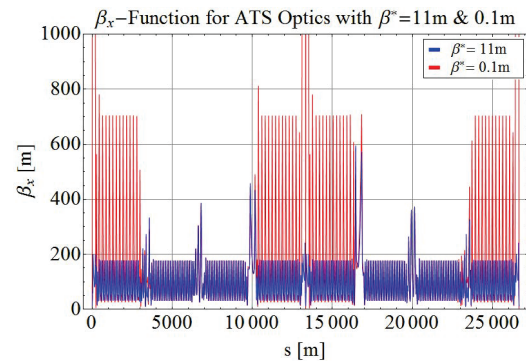


Figure 1: β -functions for ATS optics with $\beta^* = 11$ m (blue) and 0.1 m (red) in IP 1 and 5.

IBS GROWTH RATES

The IBS growth rates $\alpha_{\text{IBS},i}$ ($i = x, l, y$) in the horizontal, longitudinal and vertical plane can be written [5] as

$$\begin{pmatrix} \alpha_{\text{IBS},x} \\ \alpha_{\text{IBS},l} \\ \alpha_{\text{IBS},y} \end{pmatrix} = A \begin{pmatrix} \gamma^2 \mathcal{H}_x \\ \varepsilon_y^2 \\ \frac{\gamma}{\sigma_y^2} \\ \frac{\beta_y}{\varepsilon_y} \end{pmatrix} \times \int_0^\infty \frac{\lambda^{1/2}}{(\lambda^3 + a\lambda^2 + b\lambda + c)^{3/2}} \begin{pmatrix} [a_x\lambda + b_x] \\ [a_l\lambda + b_l] \\ [a_y\lambda + b_y] \end{pmatrix} d\lambda \quad (2)$$

*Michaela.Schaumann@cern.ch

with

$$A = \frac{r_0^2 c N_b (\log)}{8\pi\gamma(\gamma^2 - 1)^{3/2} \epsilon_x \epsilon_y \sigma_\delta \sigma_z} \quad (3)$$

and

$$\mathcal{H}_x = \frac{D_x^2}{\beta_x} (1 + \alpha_x^2) + \beta_x D_x'^2 + 2\alpha_x D_x D_x' \quad (4)$$

where γ is the relativistic factor, $\epsilon_{x,y}$ the transverse emittances, σ_z the bunch length, σ_δ the energy spread, r_0 the classical particle radius, c the speed of light, $\beta_{x,y}$ the horizontal and vertical β -function, (\log) a Coulomb logarithm and the remaining coefficients inside the integral can be found in Table 1 of [5], they depend on the optics and beam parameters. In this form the horizontal IBS growth rate $\alpha_{\text{IBS},x}$ is proportional to the horizontal \mathcal{H} -function form (4) which is plotted in Figure 2. It only depends on optics: the horizontal dispersion D_x and its derivative D_x' and the optical functions β_x and $\alpha_x = -\beta_x'/2$. The \mathcal{H} -function increases in the four arcs around the main IP for the squeezed optics (red), similar to the β -functions in Figure 1.

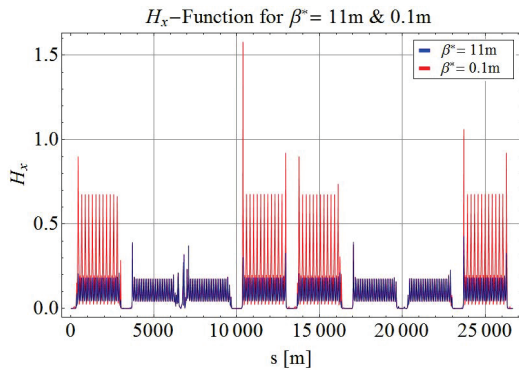


Figure 2: Horizontal \mathcal{H} -function.

In Figure 3 the local contribution of the IBS growth due to a specific element around the ring calculated with MADX is shown for the unsqueezed case ($\beta^* = 11$ m, blue) and the fully squeezed optics ($\beta^* = 0.1$ m, red). Again, the oscillations in the arcs surrounding the main IPs are enhanced for small β^* . In the horizontal plane this arises from proportionality of the IBS growth rate to the \mathcal{H} -function, in the longitudinal plane the dependence on the lattice functions is less dominant. The black and red lines represent the cumulative sum, which accumulates the local growth rates (blue and red, respectively) at each element with increasing s . They indicate that the squeeze increases the total IBS growth rate for the whole ring (maximum value of the cumulative sum) in the horizontal and slows it down in the longitudinal plane.

The evolution of this effect along the squeeze is shown in Figure 4, where the total IBS growth rate is plotted as a function of β^* for the longitudinal (dashed lines) and horizontal (solid lines) plane. The calculations were done for the beam parameters of the two possible scenarios given in Table 1. Since the bunches are expected to have a higher

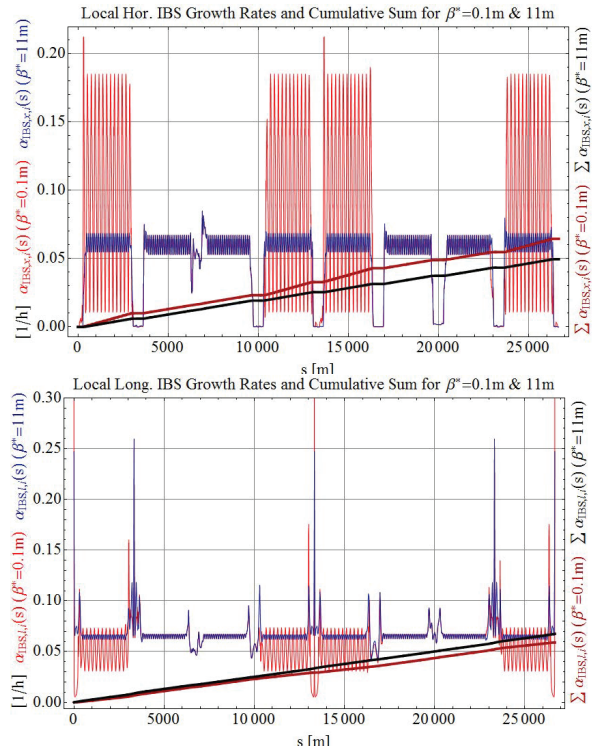


Figure 3: Local contribution of the IBS growth rates. Top: horizontal, bottom: longitudinal plane.

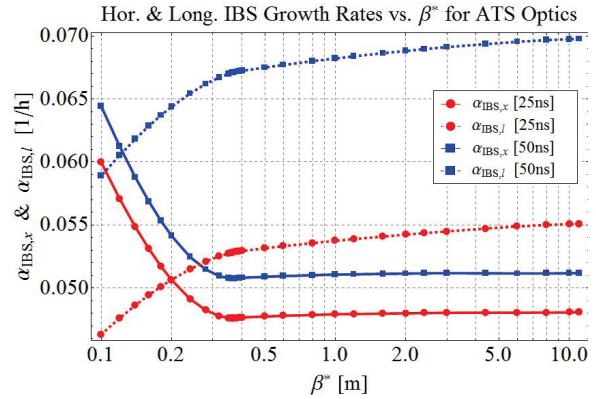


Figure 4: IBS growth rates along the squeeze.

brightness for the 50 ns case, the growth rates are also enhanced with respect to the 25 ns option.

The computations described above were done in a flat machine, without crossing angle and separation bumps. However, switching on the crossing angle bumps in the IPs enhances the dispersion, since the particles pass the triplet quadrupoles on an off-centred orbit. Dispersion is induced in both planes by the alternating crossing scheme in IP1 and 5. This can have a major influence on the stability of the beam and must be corrected. In a machine with crossing angle bumps and dispersion correction the IBS growth rates behave very similar compared to the flat machine.

Two ATS-optics versions were considered, based on the nominal sequence (ATS-V6.503 [6]) and including new

triplet magnets around the IPs (SLHCV3.1b [7]). The differences between these optics have only a marginal effect on the IBS growth rates.

Table 2 summarises the total IBS growth rates calculated with MADX at injection (450 GeV) and collision (7 TeV) energy for the nominal value of $\beta^* = 0.15$ m. See [8] for full details.

Table 2: Summary of the IBS Growth Rates

Spacing	25 ns		50 ns	
E [GeV]	450	7000	450	7000
β^* [m]	11	0.15	11	0.15
$\alpha_{\text{IBS},l}$ [1/h]	0.096	0.049	0.124	0.062
$\alpha_{\text{IBS},x}$ [1/h]	0.096	0.054	0.103	0.058
$\alpha_{\text{IBS},y}$ [10^{-4} /h]	-6.4	-0.015	-6.9	-0.016

SIMULATIONS OF THE BEAM EVOLUTION

The simulations were done with the Collider Time Evolution (CTE) program [3] using the ATS-V6.503 optics of the flat machine. The differences in IBS between the two optics versions with/without crossing angle bumps and dispersion correction are small. Figures 5 and 6 show the evolution of the luminosity and beam parameters as a function of time in collisions.

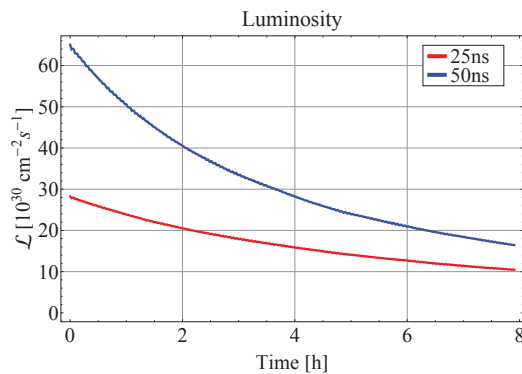


Figure 5: Simulated single bunch luminosity evolution per bunch crossing (without levelling and crab-cavities).

The red and blue lines correspond to a single bunch with the initial parameters given in Table 1 for the 25 ns and 50 ns scenario, respectively. The luminosity calculation does not include levelling or crab-cavities, it only indicates the achievable “virtual” bunch luminosity. Table 1 shows that the bunches have a higher brightness for the 50 ns option so produce a higher luminosity per bunch crossing. However the luminosity burn-off and intensity decay are faster and emittance growth is also stronger. The particle losses are dominated by the luminosity production and the debunching losses arising from IBS are estimated to be below 1% in all cases. The bunch length shrinks because of the rather strong radiation damping at 7 TeV which overcomes the counter-effect of IBS in the longitudinal plane.

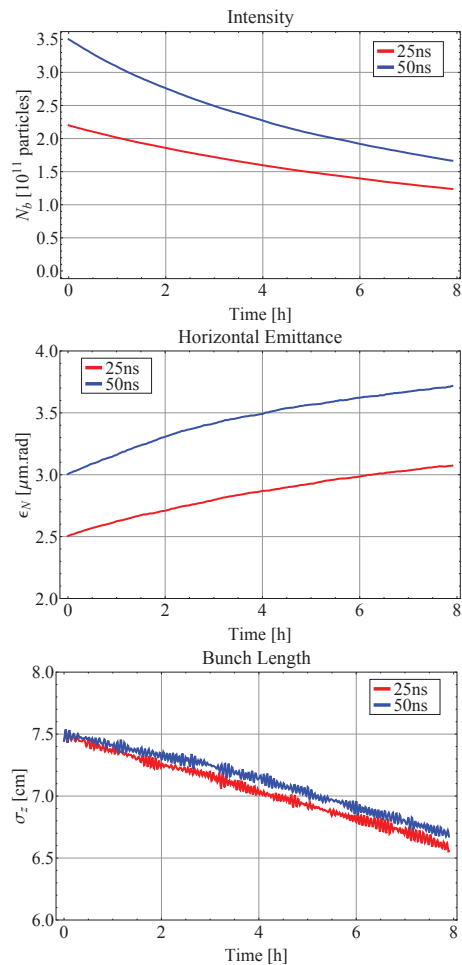


Figure 6: Simulated bunch evolution.

ACKNOWLEDGMENT

We thank R. De Maria, S. Fartoukh and E. Métral for useful discussions. MS is supported by the Wolfgang-Gentner-Programme of the BMBF (Federal Ministry of Education and Research, Germany). This work was done in the frame of Task 2.4 “Collective Effects” of HiLumi LHC Work Package 2. The HiLumi LHC Design Study is included in the High Luminosity LHC project and is partly funded by the European Commission within the Framework Programme 7 Capacities Specific Programme, Grant Agreement 284404.

REFERENCES

- [1] S. Fartoukh, CERN-ATS-2011-161.
- [2] <http://www.cern.ch/madx>
- [3] R. Bruce et al., Phys. Rev. ST Accel. Beams 13, 091001 (2010).
- [4] O. Brüning and F. Zimmermann, CERN-ATS-2012-070.
- [5] F. Antoniou and F. Zimmermann, CERN-ATS-2012-066.
- [6] S. Fartoukh et al., CERN-ATS-2012-080.
- [7] S. Fartoukh et al., CERN-ATS-2012-136.
- [8] M. Schaumann et al., CERN-ATS-2012-290.